VNU Journal of Science, Mathematics - Physics 26 (2010) 29-35

Simulation study of microscopic bubbles in amorphous alloy $Co_{81.5}B_{18.5}$

Pham Huu Kien[1,*], Pham Khac Hung[1], Vu Van Hung[2]

[1]*Department of Computational Physics, Hanoi University of Technology*

[2]*Department of Physics, Hanoi National University of Education, 136 Xuan Thuy, Cau Giay, Hanoi, Vietnam*

Received 8 September 2009

Abstract. Simulation of the diffusion mechanism via microscopic bubbles in amorphous materials is carried out using the statistical relaxation models $Co_{81.5}B_{18.5}$ containing 2×10^5 atoms. The present work is focused on the role of these bubbles for self-diffusion in amorphous solids. It was found that the numbers of the vacancy bubbles in amorphous $Co_{81.5}B_{18.5}$ vary from 1.4×10^{-3} to 4×10^{-3} per atom depending on the relaxation degree. The simulation shows the collective character of the atomic movement upon diffusion atoms moving. Due to the large size in comparison with B atom, the jump of a Co diffuses atom leads to a significant local rearrangement of the atoms located near the VB. Meanwhile, B diffuses like the movement of an interstitial impurity through the boron-VB. Diffusion coefficients have been calculated via the vacancy bubbles and they are consistent with experimental data. The effect of the relaxation is also investigated and interpreted as a result of vacancy-bubble annihilation during thermal annealing. Keywords:

Keyworks: Bubbles; Amorphous alloys; Vacancy bubbles; Diffusion mechanism; Statistical relaxation.

1. Introduction

The diffusion behavior in amorphous materials have been investigated by both experiment and computer simulation for a long time [1-23]. For amorphous alloys (AMAs), the diffusion coefficient of tracer atoms in well-relaxed specimens decreases compared to that in as-quenched ones [1-11]. Generally, the diffusivity in AMAs is interpreted as the quasi-vacancies in super-saturation is reduced during thermal annealing until the relaxation is over, and the diffusion coefficient reaches its final value. In well-relaxed state, conversely, the tracer atoms diffuse via the collective movement of a group of neighboring atoms. However, the experimental measurements [10-16] on the isotope effect, pressure dependence and irradiation-enhanced diffusivity are sometimes in contradiction to the prediction of the diffusion mechanism described above. In addition, the definition of the quasi-vacancy is not clear. Molecular dynamic (MD) simulations reveal that the vacancies are unstable in an amorphous matrix [15, 16]. In close inspection of the MD model, a continuous spectrum of small spherical voids is found in both Fe-P and Co-B models [17], but their size is less than the atomic size. Regarding the collective atomic jumps, the free volume and two-level states theories are employed to interpret the specific

* Corresponding author. E-mail: huukienpham@yahoo.com

diffusion behavior in AMAs [14-20]. However, the correlations of diffusion in amorphous $Ti_{60}N_{40}$ and $Fe_{40}Ni_{40}B_{20}$ alloys [2] show that the atomic jump process in amorphous alloys seems to be cooperative in nature; details of such process have yet to be clarified. Recently, we have reported that the evidence of microscopic bubbles has been found in amorphous $Fe_{80}B_{20}$ alloys [22]. A systematic study of these bubbles should be carried out in other amorphous systems in order to interpret the possible diffusion mechanism of tracer atoms in AMAs. This paper focus on the microscopic bubbles and the diffusion mechnism via these bubbles in AMAs $Co_{81.5}B_{18.5}$.

2. Computation procedure

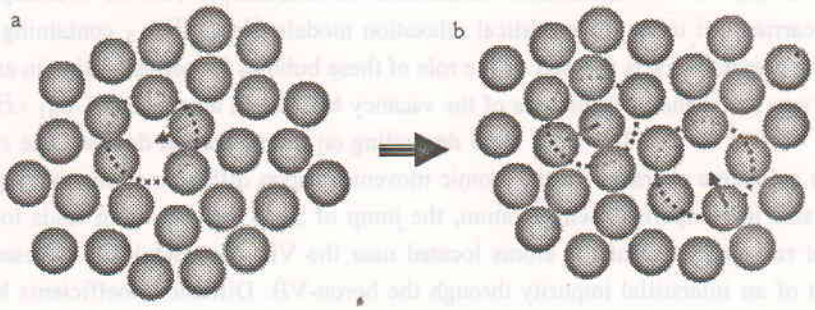

Fig. 1. The schematic illustration of bubbles in AMAs.

Amorphous models containing 2×10^5 atoms are constructed by the continuous static relaxation (SR) method. The SR method is in fact the molecular dynamic method in which the kinetic energy is equal to zero and the volume is constant. Accordingly, each atom in the system moves in the direction of the force acting on the given atom from all remaining ones by a length dr. This movement is repeated many times until the system reaches to equilibrium state. More details on the SR method can be found elsewhere [17, 22]. The initial configuration is generated by randomly placing all atoms in a cubic with periodic boundary conditions. The Pak-Doyama effective pair potential in ref. [22] is used and the density is adopted from a real amorphous alloy ($8.3g/cm^3$). This model, as called model A, is treated over 10^6 SR steps to reach the equilibrium state. The SR step length is equal to 0.01 A. The validity of the constructed model has been tested such that the pair distribution functions (PDFs) are reproduced well. To investigate the effect of relaxation, two additional models (model B and C) with the same density as the model A are constructed, but of which the potential energy is lower. The model B is constructed by relaxing the model A within 100 SR steps with a SR step length of 0.4 A. This is like shaking the atomic arrangement in the model A. Then, the model B is continuously relaxed with a SR step length of 0.01 A, until the system reaches to a new equilibrium state. This procedure is repeated many times such that the potential energy of the system attains the desired value. The model C is obtained by an analogous procedure. By using the models obtained, the microscopic bubbles are examined. The microscopic bubbles in AMAs $Co_{81.5}B_{18.5}$ are also dinoted in ref [22]. Figure 1 presents the new 5-bubble (Fig.1 b) is found in a solid after atom-DA in the old 5-bubble (Fig.1 a) is completed and new neighboring atoms.

3. Results and discussions

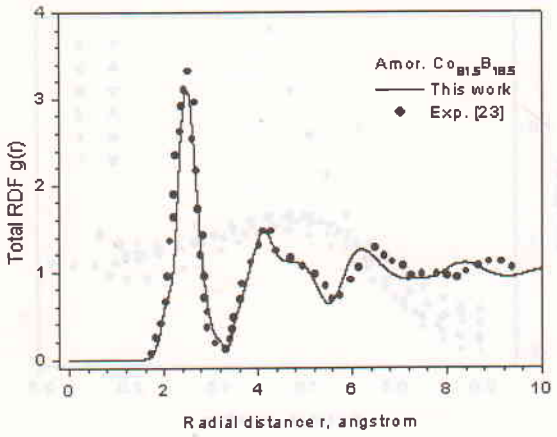

Fig. 2. The total radial distribution function of AMA $Co_{81.5}B_{18.5}$

To test the validity of the constructed models, we have compared our the obtained total radial distribution function (RDF) with experimental data. The total RDF is determined as follow:

$$g(r) = \frac{c_1^2 f_1^2 g_{11}(r) + 2c_1 c_2 f_1 f_2 g_{12} + c_2^2 f_2^2 g_{22}}{(c_1 f_1 + c_2 f_2)^2}, \quad (1)$$

where c_1 and c_2 are the concentration constants of Co and B, respectively; f_1 and f_2 are the scattering constants of Co and B, respectively; $g_{11}(r), g_{12}(r)$ and $g_{22}(r)$ are the partial RDFs of Co-Co, Co-B and B-B pairs, respectively. As observed in figure 2, the total RDF is good in agreement with the experimental data in [15, 23]. As shown in figure 2, the total RDF have a split second peak like that observed experimentally, which is thought to be related to the existence of an icosahedral form in the system. This split peak is also a typical feature for binary metal-metalloid amorphous alloys.

Table 1. The number of bubbles

Model	The mean potential energy per atom, eV	Number of atoms n_B				
		5	6	7	8	≥ 9
A	-0.91867	221633	30882	1091	159	29
B	-0.92996	214739	30231	987	125	2
C	-0.93811	211431	27196	413	51	3

The number of bubbles calculated in AMA $Co_{81.5}B_{18.5}$ models are listed table 1. As observed in table 1, all models contain more than one bubble per atom. The number of bubbles in the model decreases with the decrease of the mean potential energy per atom. This means that the well-relaxed model (model C) has a smaller number of bubbles compared to the as-quenched model (model A). This trend is also observed by the distribution of bubble radius shown in table 2. It can be seen that the number

of large bubbles, those with a radius larger than 1.5 A, in the well-relaxed model is smaller than that in the less-relaxed model.

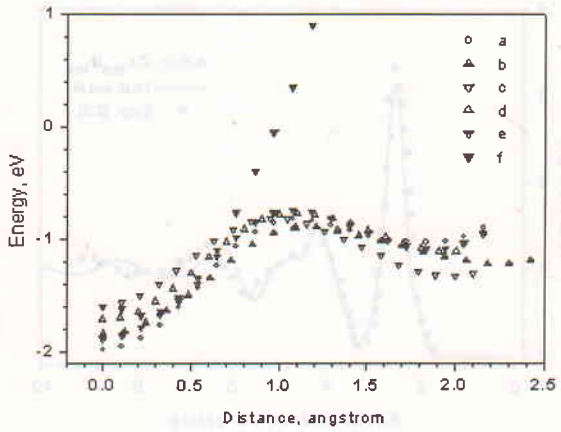

Fig. 3. Potential energy profile of atoms moving from their site to the center of the CST; a, b, c, d and e belong to VB in AMAs.

As in our previous work [21], we calculate the potential energy variation of all neighboring atoms as they move step by step on a line connecting their initial equilibrium position and the center of the CST. The potential energy profiles (PEP) for an atom moving into the bubbles are shown in figure 3. Some type-PEPs are found in the models. For the type-PEP f, the PEP increases monotonously. It indicates that the neighboring atom cannot jump into the bubble due to a very large energy barrier. For the type-PEP a, b, c, d and e, a maximum of the PEP is observed. It implies that these typical PEPs permit a tracer atom jumping into the bubbles. The bubbles with the neighboring atoms having the type-PEP a, b, c, d and e play a role as a diffusion defect like a vacancy in crystal. These bubbles are called vacancy bubbles (VB). The atoms attaining the type-PEP a, b, c, d and e are called the diffusing atom (DA). The number of VBs in the models is presented in table 3. There are two kinds of VBs: cobalt- and boron-VB corresponding to the cobalt- and boron-DA, respectively. As listed in table 3, the number of both n_{Co}- and n_B-VB in the less-relaxed model is larger than that in the well-relaxed model.

Figure 4 shows the distributions of site energy and potential barrier height for DAs. The potential barrier height is determined by the difference between the maximum point of the PEP and the site energy of DAs. These distributions, for all models considered, have a Gaussian form. The well-relaxed model has the higher peak compared to the less-relaxed model.

In order to inspect the collective atomic movement of atoms in AMA $Co_{81.5}B_{18.5}$ upon DA moving, the DA is displaced into the center of the CST after the VBs are determined. Then, the system is relaxed until it reaches a new equilibrium. This process is called \the DA moving}. Table 3 presents the mean square displacements after the DA moving completed, and the x^2_{Co} and x^2_B for the individual ith run are shown in figure 5. In the model C, the mostly fluctuates around 4.3 A for the boron-DA while it decreases closely to zero in the case of the cobalt-DA. Due to jumping distance of the DA in the range of 1.6 to 1.9 A the boron-DA contributes the dominant part of x^2_{Bi} e.g. other B atoms move

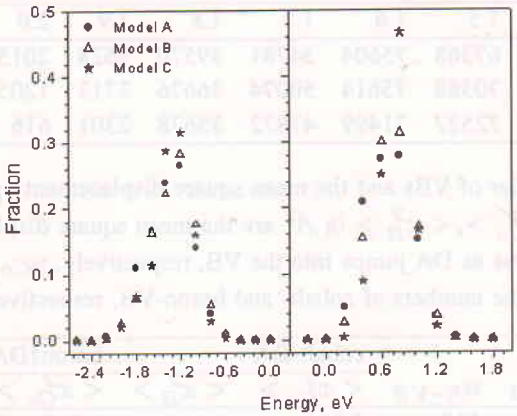

Fig. 4. The distributions of site energy (left) and energy barrier (right) for DAs.

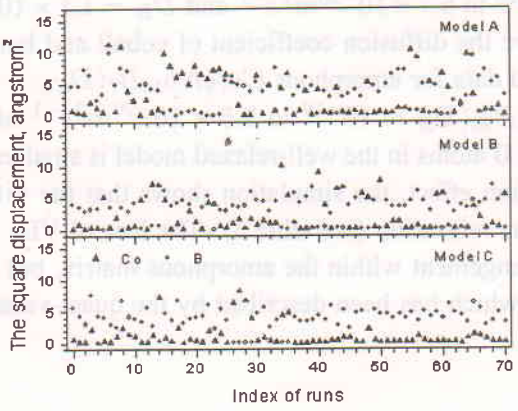

Fig. 5. The square displacements of Co and B atoms, x^2_{Coi} and x^2_{Bi} for the ith run of DA moving.

not far from their initial positions under the DA moving. In contrasted with the model C, the value of x^2_{Coi} in model A and B is significantly larger than 4.3 A and sometimes reaches to 14 A for the case of cobalt-DA. This result shows the collective character of the atomic movement is mainly related to cobalt-DA moving. Due to the large size in comparison with B atom, the jump of a Co atom leads to a significant local rearrangement of the atoms located near the VB. Meanwhile, boron diffuses like the movement of an interstitial impurity through the boron-VB. As such, the microscopic VBs play a role like meaning in the case of diffusion in crystal, and the diffusion mechanism performed as follows: one DA (Co or B) jumps into a VB and the present VB disappears, but another VB may be created somewhere in an amorphous matrix due to the collectively atomic movement upon DA moving (see figure 1). A result of collective movement of a group of atoms is that some bubbles become VBs. These VBs are unlike the quasi-vacancies described in [4-6] which move over a certain distance until they are annihilated at a source.

Table 2. The radii distribution of bubbles

R_B, A	1.4	1.5	1.6	1.7	1.8	1.9	2.0	2.1	≥ 2.2
Model A	8316	67368	75604	54781	39570	5628	2015	350	162
Model B	8308	70368	75614	50074	36676	3713	1205	242	39
Model C	8509	72527	71499	47872	35678	2301	616	85	7

Table 3. The number of VBs and the mean square displacement upon DA moving. Here $< x_{Co}^2 >, < x_B^2 >$ in A^2 are the mean square displacement of Co and B atoms as DA jumps into the VB, respectively; n_{Co-VB}, n_{B-VB} are the numbers of cobalt- and boron-VB, respectively

			cobalt-DA		boron{DA	
Model	n_{Co-VB}	n_{B-VB}	$< x_{Co}^2 >$	$< x_B^2 >$	$< x_{Co}^2 >$	$< x_B^2 >$
A	249	538	8.951	1.164	1.834	4.947
B	95	354	6.107	0.193	0.807	4.332
C	46	236	6.202	0.184	0.576	4.301

The diffusion coefficient of the models is calculated as denoted in [21]. From the simulation data, we get $D_{Co} = 1.5 \times 10^{-20}$ to $6.7 \times 10^{-20} m^2 s^{-1}$ and $D_B = 1.1 \times 10^{-19}$ to $3.9 \times 10^{-19} m^2 s^{-1}$ at 593 K, where D_{Co} and D_B are the diffusion coefficient of cobalt and boron, respectively. This result is consistent with experimental data for amorphous $Co_{79}Nb_{14}B_7 (D_{Co} \sim 10^{-20}$ to $6.5 \times 10^{-23} m^2 s^{-1}$ at 663 K) [10], and $Fe_{40}N_{40}B_{20} (D_B \sim 10^{-19}$ to $3.5 \times 10^{-20} m^2 s^{-1}$ at 593 - 600 K)[3, 22]. The diffusion coefficient of Co and B atoms in the well-relaxed model is smaller than that in the less-relaxed model. As regards the relaxation effect, the simulation shows that the diffusion coefficient decreases due to the loss of VBs upon the relaxation (see table 3). The loss of VBs in the well-relaxed model is concerned with the atomic arrangement within the amorphous matrix, but not due to the source where the diffusion effect moves to, which has been described by the quasi-vacancy models [1-4].

4. Conclution

The structure of amorphous $Co_{81.5}B_{18.5}$ models containing 2×10^5 atoms with the Pak-Doyama effective potentials is in good agreement with the experimental data. A large number of VBs are found in these models. It is in the range from 1.4×10^{-3} to 4×10^{-3} per atom depending on the relaxation degree. The VB could be a diffusion vehicle as a vacancy in the crystal i.e. one DA in the VB could move into the CST and present an elemental diffusion jump. In other works, a new diffusion mechanism is presented in that a DA jumps into the VB, then the collective movement of neighboring atoms starts. Consequently, the present VB disappears, but another VB may be created somewhere in the amorphous matrix. The diffusion coefficients of Co and B atoms are calculated via the VBs detected, and the result is consistent with the experimental data. The decrease in the diffusivity upon the relaxation results in the VB annihilation. This indicates that the VB is unlike the quasi-vacancy, which is previously used to interpret the relaxation effect.

Acknowledgments. This work was supported financially by a cluster system with 50 PC nodes at the High Performance Calculation Center, Hanoi University of Technology.

References

[1] J. Horvath, J. Ott, K. Pfahler, W. Ulfert, *Mater. Sci. Eng*, 97 (1988) 409.
[2] J. Pavlovsky, W. Ulfert, W. Frank, *Mater. Chem. Phys*, 36 (1994) 383.
[3] W. Frank, A. Horner, P. Scharwaechter, H. Kronmiiler, *Mater. Sci. Eng*, 97 (1988) 415.
[4] A. K. Tyagit, M.P. Macht, V. Naundorf, *Acta Metall, Mater* 39 (1991) 609.
[5] T. Schuler, *NanoStruct. Mater*, 6 (1995) 863.
[6] S. Flege, U. Fecher, H. Hahn, *J. Non-Cryst. Solids*, 270 (2000) 123.
[7] A. Griesche, *Mater. Sci. Eng*, A 375 (2004) 285.
[8] A. van den Beukel, J. Sietsma, *Mater. Sci. Eng*, A 134 (1991) 935
[9] S.K. Sharma, S. Banerjee, Kuldeep, A.K. Jam, *Acta Metall* 36 (1988) 1683.
[10] J. Du Plessis, G. N. van Wyk, *Appl. Surf. Sci* 40 (1990) 303.
[11] Y. Limoge, *J. Non-Cryst. Solids* 117-118 (1990) 708.
[12] Y. Limoge, *Acta Metall. Mater* 38 (1990) 1733.
[13] R.S. Averback, *MRS Bulletin* 16 (1991) 47.
[14] Y. Limoge, *Mater. Sci. Eng* A 226-228 (1997) 228.
[15] P.K. Hung, H.V. Hue, L.T. Vinh, *J. Non-Cryst. Solids* 352 (2006) 3332.
[16] A. Zhu, G.J. Shiflet, S.J. Poon, *Acta Materialia* 56 (2008) 3550.
[17] D. Leon et al., *Mater. Sci. Eng* A 226-228 (1997) 296.
[18] V. Naundorf et al., *J. Non-Cryst. Solids*, 224 (1998) 122.
[19] B.K. Belashchenko, V.V. Hoang, P.K. Hung, *J. Non-Cryst. Solids*, 276 (2000) 169.
[20] G.S. Chadha et al., *Phys. Stat. Sol*, A 63 (2) (1981) 625.
[21] P.K. Hung, P.H. Kien and L.T. Vinh, *J. phys.: Condens. Matter*, 22 (2010) 035401.
[22] W. Ulfert et al., *Cryst. Latt. Deft Amorph. Mater*, 18 (1989) 519.
[23] P. Lamparter et. al., *Z. Naturforsch*, 6 (1981) 165.